Suomi-NPP VIIRS Initial Reprocessing Improvements and Validations in the Reflective Solar Bands

Taeyoung Choi[1,3*], Junqiang Sun[2,3], Bin Zhang[1,4], Zhuo Wang[4], Changyong Cao[3], Fuzhong Weng[3], Menghua Wang[3]

[1]Earth Resources Tech. Inc., [2]Global Science and Technology, [3]NOAA Center for Satellite Applications and Research (STAR), [4]University of Maryland

ABSTRACT

Over five years of the Suomi National Polar orbiting Partnership (S-NPP) Visible Infrared Imaging Radiometer Suite (VIIRS) Sensor Data Records (SDR) production, there were mutual demands of the lifetime VIIRS SDR reprocessing to alleviate operational changes and user oriented suggestions. Meanwhile, the NOAA Ocean Color (OC) team through its independent effort has achieved the robust calibration of the S-NPP VIIR Reflective Solar Bands (RSBs) – including improved radiometric accuracies, minimized annual oscillations and mitigated growing bias for long-term radiometric stability. The baseline VIIRS reprocessing is performed using the RSBAutoCal LUTs with an option of using OC calibration for their mission-long reprocessing to provide enhanced radiometric accuracy for OC Environmental Data Records (EDR) products. The SDR reprocessing team has applied the most recent calibration coefficients LUTs from the RSBAutoCal processing unit as a baseline product with a new field called 'RadiometricBaisCorrection,' which holds conversion factor from baseline to OC's suggested calibration. This paper briefly summarizes the efforts of the SDR reprocessing team, the related entire life reprocessing issues and the initial results in the RSBs. It will show that the quality and accuracy of the SDR reprocessed with the new LUTs are significantly improved. It will also demonstrate the remarkable improvements of the VIIRS EDR for various applications and higher-level science products by using the reprocessed SDR as their inputs.

Keywords: S-NPP, VIIRS, RSB, SDR, Reprocessing, LUT

1. INTRODUCTION

The Suomi National Polar-orbiting Partnership (S-NPP) satellite was launched on October 28th, 2011 with a major Visible Infrared Imaging Radiometer Suite (VIIRS), among other four sensor such as Cross-track infrared Sounder (CrIS), Advance Technology Microwave Sounder (ATMS), Ozone Mapping Profiler Suite (OMPS), and Clouds and the Earth's Radiant Energy System (CERES). Detailed calibration and validation study, scientific data products of these instruments were discussed and published in special issue of 'S-NPP Calibration and Validation Scientific Results' with the Journal of Geophysical Research at http://onlinelibrary.wiley.com/journal/10.1002/(ISSN)2169-8996/specialsection/SNPPCVSR1. With a nominal altitude of 824 km, the S-PP is in a sun-synchronous orbit in an ascending node with the equator passing time of 1:30 p.m. [1][2]. The VIIRS can provide the entire Earth observations since the S-NPP satellite orbits the Earth approximately 14 times per day with the scan swath of about 3000 km. To meet the scientific data quality, VIIRS uses improved sensor and on-board calibrators which have back traceability to the prelaunch calibration references. Based on lessons learned from the Moderate resolution Imaging Spectroradiometer (MODIS) design, VIIRS has the Half Angle Mirror which de-rotates incoming radiation path of the Rotating Telescope Assembly (RTA). Along with the RTA scan path, the VIIRS instrument has a series of On-Board Calibrators (OBC) such as blackbody (BB), Solar Diffuser (SD), Solar Diffuser Stability Monitor (SDSM), and Space View (SV). The VIIRS has 20 narrow spectral bands with one Day Night Band (DNB) with broad spectral response. These VIIRS spectral bands are listed in Table 1 with the corresponding Center Wavelengths (CW) except the DNB [2].

*Primary author: taeyoung.choi@noaa.gov; phone 1-301-683-3562; STAR / NESDIS / NOAA

Earth Observing Systems XXII, edited by James J. Butler, Xiaoxiong (Jack) Xiong, Xingfa Gu, Proc. of SPIE Vol. 10402, 104021V · © 2017 SPIE · CCC code: 0277-786X/17/$18 · doi: 10.1117/12.2274081

Table 1. VIIRS Spectral Bands without DNB

	Reflective Solar Bands (RSB)													
	VisNIR									SWIR				
Band	M1	M2	M3	M4	I1	M5	M6	I2	M7	M8	M9	I3	M10	M11
CW [nm]	411	444	486	551	639	672	745	862	862	1238	1375	1602	1602	2257

	Thermal Emissive Bands (TEB)						
	MWIR			LWIR			
Band	I4	M12	M13	M14	M15	I5	M16
CW [μm]	3.753	3.697	4.067	8.578	10.729	11.469	11.845

For the RSB, the primary source of calibration is based on the SD observations. Because of the SD reflectance changes especially in the short wavelengths, the long-term monitoring and correction of the SD degradation is key factor for the RSB calibration, which is monitored by the Solar Diffuser Stability Monitor (SDSM). The simplified schematics of all these OBCs, RTA, and opto-mechanical models are shown in Figure 1. For the RSB calibration, there were some calibration updates such as H-factor updates and C0=0 update which caused sudden changes of radiometric values in the Sensor Data Records (SDR) [3].

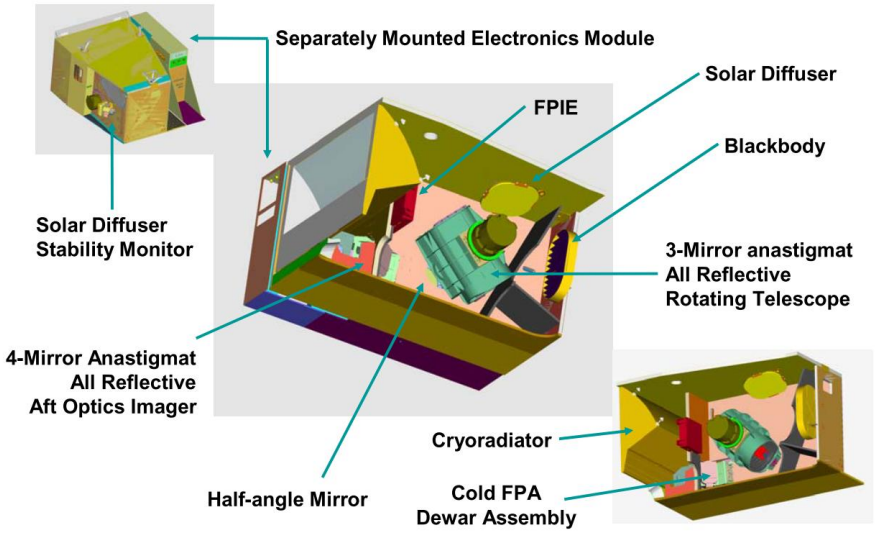

Figure 1. VIIRS schematic with on-board calibrators and Opto-Mechanical Module [4].

On the contrary, TEB calibration has been very stable due to very stable V-grooved blackbody (BB) temperature at 292.5K. To measure calibration coefficient changes, there has been BB Warm-Up-Cool-Down (WUCD) cycles every three months. The BB WUCD cycle requires approximately 3 days and calibration anomalies have been observed from the NOAA Sea Surface Temperature (SST) group. During the WUCD cycles, SST group found coincident global warming on the order of 0.3K along with the BB WUCD periods. To resolve these periodical global SST problems, a empirical gain correction is suggested initially [5] and finally Ltrace method has been developed which was based on operational algorithm analysis[6]. The Ltrace method improved WUCD F-factor anomalies especially in bands M15 and M16, which was validated by matching the CrIS observations.

Due to the RTA tungsten degradation, the DNB Relative Spectral Response (RSR) has been continually changed especially in early lifetime. To compensate the RSR changes, current NOAA Interface Data Processing Segment (IDPS)

production system only applied one time RSR update on April 5th, 2013. In addition to these RSR changes, there were previous DNB calibration algorithm updates in 2012 [7]. In addition, the IDPS VIIRS DNB products were not matured because of the missing bias and offset tables. Another issue in the DNB product was the stray light issues near the day and night transition areas. The DNB stray light correction became operational in August of 2014. The VIIRS DNB SDR granules include straylight problems near the day and night transition areas.

Based on the above RSB, TEB and DNB issues, there have been user oriented request of the entire lifetime reprocessing of VIIRS SDR. This study is going to focus on RSB calibration issues with SD calibration coefficients, mitigation strategies, and SDR radiometric improvements after reprocessing. In section 2, the standard RSB calibration algorithm using SD and SDSM is briefly reviewed. In section 3, NOAA OC group's RSB calibration is explained. In Section 4, S-NPP VIIRS lifetime reprocessing improvements are discussed. The summary of study is shown in section 6.

2. STANDARD ON-ORBIT RSB CALIBRATION

About On-orbit RSB SD and SDSM functions

Details of on-orbit RSB calibration equation development and descriptions are well documented in the Joint Polar Satellite System (JPSS) VIIRS radiometric calibration algorithm theoretical basis document (ATBD) [4]. As a differentiating radiometer, the VIIRS continuously observes the SV to determine the bias at zero radiance condition. The primary source of calibration is the SD illumination from the Sun with its Bi-directional Reflectance Function (BRF), which was determined by prelaunch and on-orbit yaw maneuvers [8]. The on-orbit SD is made of Spectralon™ (one type of fluoropolymer) and modifies (or degrades) with the exposure to the Sun illumination. The SD degradation is monitored by the SDSM under the assumption of near Lambertian surface of the SD reflectance property especially near the angles of SDSM SD and RTA views. Analysis of VIIRS SD reflectance data show that the spectral dependent degradation of SD reflectance in short wavelength can be explained with a SD Surface Roughness (length scale << wavelength) based Rayleigh Scattering (SRRS) model due to exposure to solar UV radiation and energetic particles [9][10]. When S-NPP from the night to day side near the South Pole, the SD panel becomes illuminated by the Sun. At the same time, the SDSM Sun view port also illuminated by the Sun through a separate SDSM attenuation screen for about 1 minute. Figure 2 shows a simplified schematic of RTA, SDSM and SD along with SD and SDSM screens in the VIIRS scan cavity.

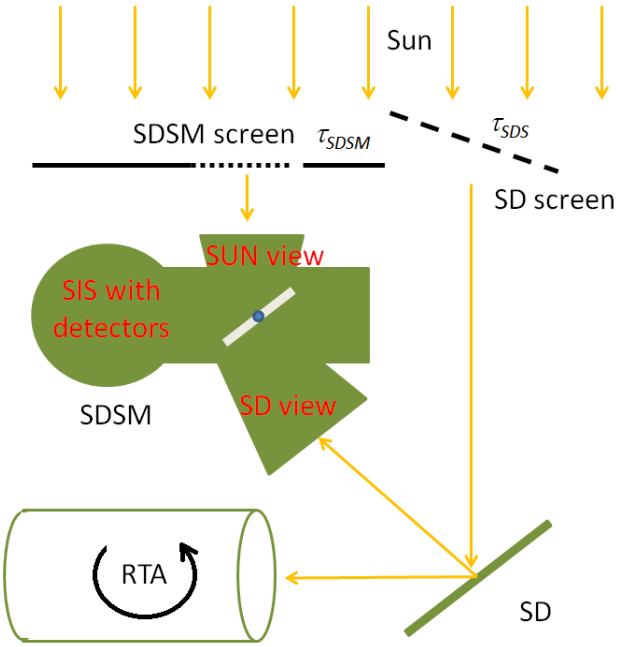

Figure 2. A simplified RTA, SDSM, SD and RTA diagram with SD and SDSM screens. The SDSM has rotating mirror to select SUN, SD or dark view responses with the detectors in the Spherical Integrating Sphere (SIS).

RSB F-factor calculation

A set of desired angle ranges for a proper Sun illumination on the SD is called a 'sweet spot' and it is defined by solar declination and azimuth angles. The standard sweet spot solar declination angle is from 14.00 to 18.39 degrees and the corresponding solar azimuth angle is from 13.6 0to 30.78 degrees [4]. On orbit F-factor (or calibration coefficient) can be derived by Equation 1 for each valid SD observation.

$$F = \frac{\cos(\theta_{inc}) \cdot \left[E_{sun} \cdot \tau_{sds} \cdot BRF_{SD}(t)\right] \cdot RVS_{SD}}{c_0 + c_1 \cdot dn_{SD} + c_2 \cdot dn_{SD}^2} \quad (1)$$

In Equation 1, θ_{inc} is solar incident angle to the SD screen, E_{sun} is solar irradiance, τ_{sds} is screen transmittance, BRF_{SD} is the SD BRF from the early lifetime yaw maneuvers, RVS_{SD} is response versus scan, $C_{0,1,2}$ are detector and electronics temperature effect corrected prelaunch radiometric coefficients. The dn_{SD} is bias corrected SD digital number from the SV.

RSB H-factor calculation

The SD BRF function changes over time because of the SD degradation and it is called H-factor. To measure the H-factor, the SDSM measures digital counts (DC) from the Sun, SD, and dark observations near simultaneously as shown in Figure 1. The SDSM includes a Spherical Integrating Sphere (SIS) with eight different detectors which receive illuminations guided by the rotating mirror. The mirror continuously moves the three positions for SD, SDSM, and dark observations within the sweet spot period. Based on the bias removed SD and Sun measurements, the H-factor is calculated by Equation 2.

$$H(t) = \frac{dc_{SD} \cdot \tau_{SDSM}}{dc_{SUN} \cdot BRF_{SDSM\_SD} \cdot \tau_{SDS} \cdot \cos(\theta_{inc}) \cdot \Omega_{SDSM}} \quad (2)$$

In Equation, the τ_{SDSM} is the Sun screen transmittance and dc_{SD} is the bias removed *DC* of the *SD* view in the numeration. In the denominator, dc_{SUN} is the bias removed *DC* of the *Sun* view, τ_{SDS} is the SD screen transmittance function, BRF_{SDSM_SD} is the *BRF* at the SDSM viewing angle to the SD panel, and Ω_{SDSM} is the solid angle of the SD view. The H-factor is normalized to the first point to find time dependent BRF function as shown in Equation 3.

$$BRF_{SD}(t) = \frac{H(t)}{H(t_0)} \cdot BRF_{SD}(t_0) \quad (3)$$

In this section, brief explanations of the standard VIIRS RSB calibration coefficients, F and H-factors, are provided based on the VIIRS ATBD. As a baseline RSB reprocessing calibration, the official implementation is used and it is known as RSBAutoCal. The RSBAutoCal is currently included in the Algorithm Development Library (ADL) package and it is also a part of the NOAA's operational Interface Data Processing Segment (IDPS).

3. OC IMPROVED ON-ORBIT RSB CALIBRATION

As shown in Eqs. (1)-(3), the accuracy of the VIIRS RSB calibration using the SD and SDSM strongly depends on that of the bidirectional reflectance factor (BRF) of the SD and that of the vignetting functions (VFs) of the screens placed in the front of the SD port and the SDSM Sun view port, through which the SD and SDSM are illuminated respectively by the Sun [9][11]. Any inaccuracy in the BRF or the VFs brings out an annual oscillation. Sun and Wang have carefully derived the BRF and the VF [9]. They have introduced dual "sweet spots" in SDSM calibration and a carefully selected "sweet spot" in SD calibration, and refined data processing procedures to further improve to reduce the noise in the derived H-Factors and F-factors [9] [11]. They have also carefully analyzed the differences of the SD degradation before and after nadir door open in early mission [11]. With these improvements, both short-term and long-term stability and high accuracy of the F-factors are obtained [9]. However, Sun et al found that the SD degrades non-uniformly with respect to both incident and outgoing directions, thus invalidates the key assumption in the SD/SDSM calibration methodology that the SD degradation in the outgoing direction towards the SDSM can be used interchangeably with the result for the outgoing direction towards the RTA [12]. The actual discrepancy results in a long-term bias in the calibration coefficients derived from the SD calibration, especially for short wavelength bands [11][12].

Same as MODIS instruments [13], SNPP VIIRS has been scheduled to view the Moon approximately monthly since launch [14][15], which provides another alternative calibration source for VIIRS RSB. The lunar calibration does not have the long-term bias issue since the reflectance of the lunar surface is very stable in the VISible (VIS) and Near-InfraRed (NIR) spectral range [14][15]. However, the accuracy of the calibration strongly depends on that of view geometric effect correction. Any error in the correction induces a seasonal oscillation in the calibration coefficients derived from the lunar calibration [15]. In addition, lunar calibration can only be implemented about nine months each year. With careful correction of the geometric effect, stable and clean RSB calibration coefficients can be derived from the lunar calibration [14][15]. In general, the derived lunar F-factors are consistent with those derived from the SD/SDSM observations [15]. However, there are observable differences between the lunar and the SD F-factors [15][16][17]. For VIIRS, the AOI of the SD on the HAM exactly coincides with that of the SV. Thus, the SD/SDSM calibration and the lunar calibration should in principle provide the same on-orbit changes over time. Considering the potential bias of the SD F-factors due to the temporal non-uniformity of the SD degradation, the lunar calibration should provide a reliable long-term calibration baseline [15]. Nevertheless, the monthly lunar observations are infrequent and unavailable for several months of the year due to a spacecraft roll angle safety constraint preventing a lunar view through the space view port [14]. Sun and Wang have developed a hybrid approach to appropriately combine SD-based and lunar-based calibration coefficients to generate a set of hybrid calibration coefficients, leading to overall stable short- and long-term calibrated VIIRS RSB Sensor Data Records (SDR) [15][18].

The ocean color EDR products are highly sensitive to the accuracy of the RSB calibration and can also be used to check the RSB calibration accuracy itself especially in the low part of the dynamic range [19]. Significant long-term drifts and unexpected features have indeed been discovered in the VIIRS normalized water-leaving radiances from the short wavelength bands and the VIIRS chlorophyll-a calculated using the NOAA Interface Data Processing Segment (IDPS) SDR [18][19], which are the current official SDR products produced using the SD F-factors. The application of the reprocessed SDR with OC's best and latest improved SD F-factors does significantly improve the quality of the ocean color EDR products due to removal of the seasonal oscillations and other errors in the SD calibration coefficients [9][18][15], but still fails to address the long-term drifts present in the products. The hybrid F-factors finally remove the long-term drifts observed in the ocean color EDR and meet the ocean color EDR's stringent requirement for the RSB calibration [18][15]. Preliminary results of the performance of the ocean color EDR with the hybrid F-factors-implemented SDR have been reported in our previous works [19].

The OC LUTs used in this reprocessing are produced with the hybrid approach applied to all RSBs (I1-I3 and M1-M11). Compared to RSBAutoCal LUTs, the OC LUTs have no artificial seasonal oscillations and much smother. They also have long-term differences, especially for short wavelength bands (M1-M4 and I1). These long-term differences remove the long-term drifts in the current IDPS SDR products and as well as those in the SDR products produced with RSBAutoCal LUTs and then those in the EDR products as demonstrated in the ocean color EDR, which is most sensitive to the accuracy of the SDR and then that of the RSB calibration.

4. S-NPP VIIRS RSB SDR OPERATION CHANGES AND REPROCESSING IMPROVEMENTS

Major VIIRS SDR Algorithm Changes with ADL (or IDPS) for current operational products

The ADL has been used for the data processing or algorithm developments for Suomi NPP. The library includes the operational algorithm which is identical to the NOAA's operational production system and it is periodically improved by the algorithm updates. The routine algorithm integration works and configuration managements are supported by STAR Algorithm Integration Team (AIT) and they support ADL environment testing and validation to implement the algorithm changes. The chronological major changes of the VIIRS SDR algorithm are shown in Figure 1. The VIIRS SDR product was achieved the 'Validate' status since April 16, 2014 followed by the 'Provisional' and 'Beta' maturity status on March 13, 2013 and May 2, 2012, respectively. These beta and provisional status indicates that the initially produced S-NPP VIIRS data were produced with the best calibration coefficients at the time of production; however, it needs to be reprocessed with the current improved calibration parameters later. In Figure 3, the RSB related changes are indicated as green color. These sudden algorithm changes are mostly captured by the RSB F-factors except the H-factor sudden changes in 2014.

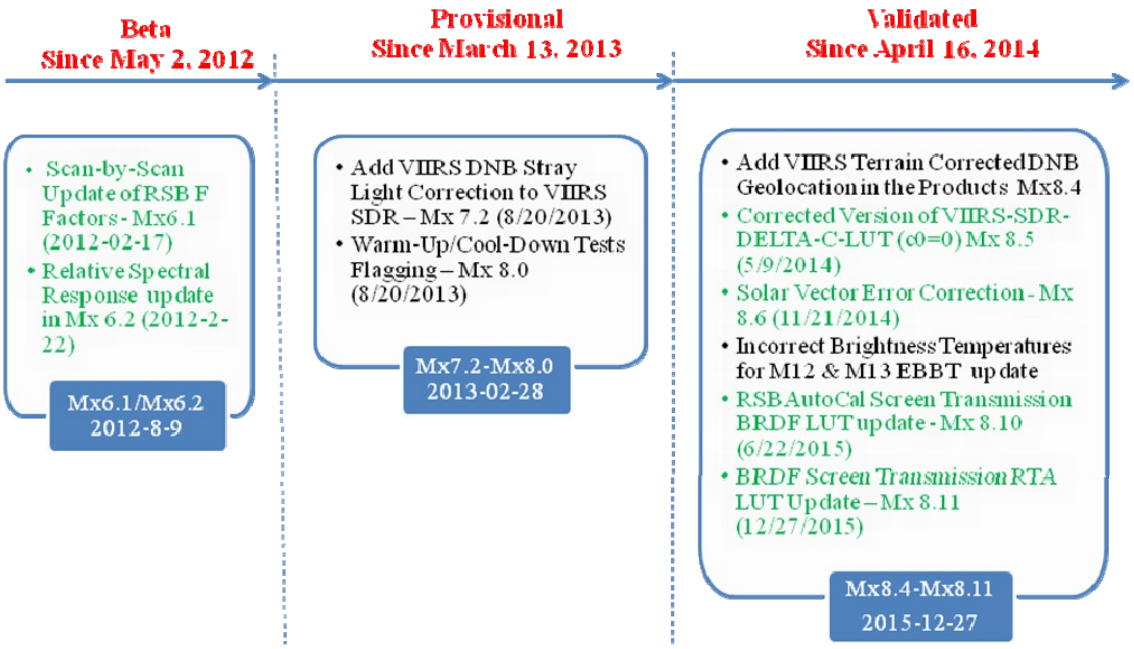

Figure 3. S-NPP VIIRS SDR processing major algorithm changes for ADL and IDPS [20].

VIIRS operational RSB F-factors changes

The VIIRS Earth View (EV) radiance values are directly related to the RSB F-factors as shown in Equation 4.

$$L_{EV} = \frac{F \cdot (c_0 + c_1 \cdot dn_{EV} + c_2 \cdot dn_{EV}^2)}{RVS_{EV}} \tag{4}$$

As a result of this linear relationship, any short-term sudden changes or long-term biases in the RSB F-factor introduce the error in the EV radiometry. In early lifetime of VIIRS, the RSB F-factors were not optimally fitted since there was no historical SD degradation or F-factor trending result for the best prediction. These unstable RSB F-factors are shown in Figure 4 especially in the short wavelength bands from M1 to M4. The operational fast-track F-PREDICTED LUTs are

shown as symbols which holds the F-factors for each band, gain state, detector, and HAM sides with slope values for the future prediction.

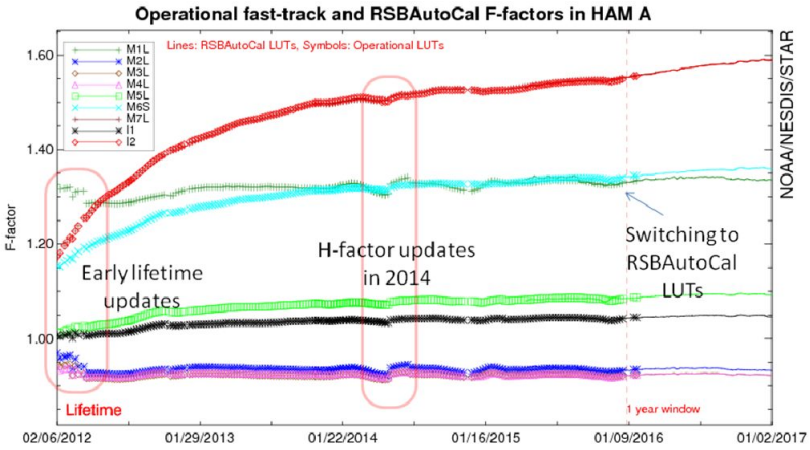

Figure 4. S-NPP VIIRS fast-track F-PREDICTED LUTs in symbols and RSBAutoCal LUTs with the solid lines. The F-factor changes are observed with algorithm updates and H-factor sudden changes in 2014.

In 2014, the SD degradation trend has been flattened approximately from Feb 2nd to May 29th. To compensate these sudden flattening of H-factor (or SD degradation), the H-factors are updated on May 23rd and July 11 accordingly [3]. Because of these H-factor sudden updates, there were sudden F-factor discontinuity points in Figure 4 around 2014. The largest changes were observed in band M1 about 1.5 percent affecting mostly short wavelength bands from M1 to M4.

In addition to the F/H-factor changes, there was delta C0 coefficient updates in 2014. The C coefficients are used in the F-factor calculation in Equation 1 and EV radiance retrieval in Equation 4. The C0 values were set to zero in all the RSB bands and the C2 (non linear coefficient) values were re-derived from the prelaunch test results. The C0=0 update was applied to the production system as of May 9th, 2014. The F-factor changes due to the C0 equal to zero update were mostly less than 0.5 percent in all the RSB bands except band I3, which showed approximately up to 1 percent change as shown in Figure 5.

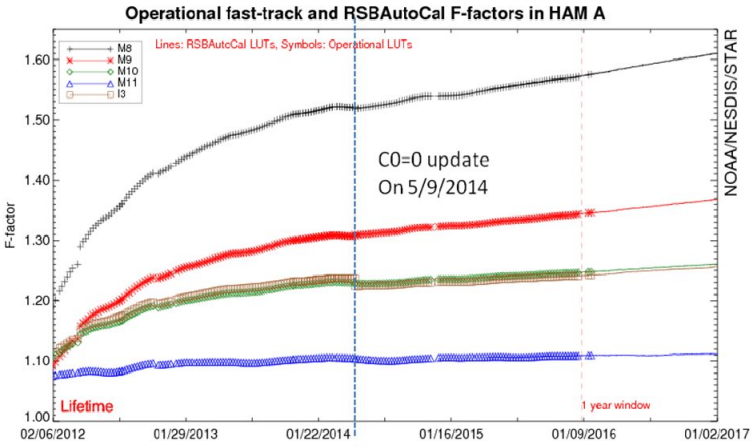

Figure 5. S-NPP VIIRS RSB C0=0 updates on May 9th, 2014.

VIIRS RSB SDR reprocessing improvements

As a baseline, the VIIRS RSB radiometric calibration coefficients (or F-factors) were recalculated using the ADL software version 4.2 which includes version Mx8.11 of the IDPS code. A flow chart of the ADL processing is shown in Figure 6. The blue boxes show the ADL processing blocks and the green boxes represents input and outputs of the ADL. The process starts with the RDRs (Raw Data Records) that are obtained from the NOAA CLASS (Comprehensive Large Array-data Stewardship System) or JPSS GRAVITE (Government Resources for Algorithm Verification Independent Testing and Evaluation) system. The major benefits of using RSBAutoCal are it is fully automatic, it frequently updates the F-factors (14 or 15 orbits per day), it is free from human errors and it reduces cost of calibration by automation.

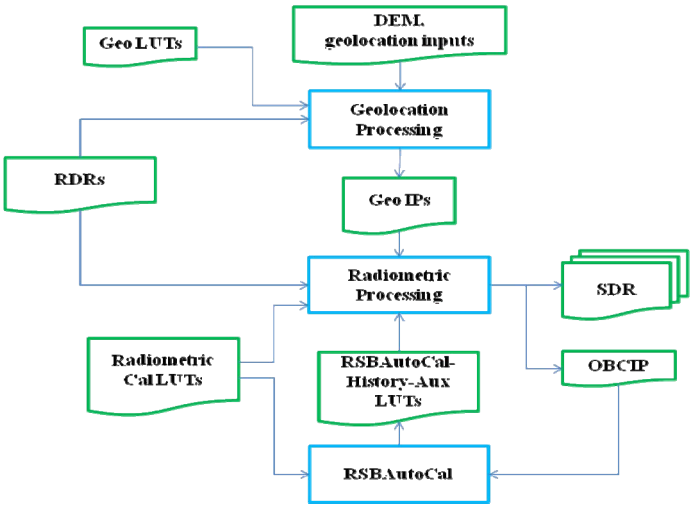

Figure 6. S-NPP ADL processing diagram for RDR to SDR generation.

The ADL radiometric processing block generates the SDR and OBCIP (On-Board Calibration Intermediate Product) which becomes an input to the RSBAutoCal. Then RSBAutoCal generates updated RSBAutoCal-History-Aux LUT that contains updated SD F-factors. This newly updated LUT is used for VIIRS radiometric process before detection of a new RSBAutoCal-History-Aux LUT. There are major improvements using the RSBAutoCal as a baseline VIIRS RSB calibration [21].

- The prelaunch calibration coefficients are updated with C0 equal to zero to improve SDR performance especially at low radiance [22].
- The error in the solar vector calculation software in the IDPS code caused by the mixed use of reference frame J2000 and time-of-date (TOD). The correction of the software introduces up to 0.2 degrees correction in the solar vector [23].
- The solar screen transmittance LUT was updated based on reanalysis of the on-orbit yaw maneuver and three years of operation onboard calibrator measurements [24].
- The H/F-factor filtering of the RSBAutoCal was improved by using RHW (Robust Holt-Winters) filtering [25].

The reprocessed band M2 and M4 high gain and HAM side A SD F-factors are shown in Figure 7. The red solid line represents current IDPS operational F-factors and it was switched to the RSBAutoCal F-factors in pink solid line starting from Nov. 2015. The reprocessed RSBAutoCal F-factors are shown as a green solid line and the OC F-factor LUT is in the blue solid line. The reprocessed RSBAutoCal F-factors (green line) successfully corrected the F-factors changes mentioned above; however, there are still annual oscillations remained after the reprocessing as shown in Figure 7. The bands M2 and M4 have the largest differences between the reprocessed RSBAutoCal and OC LUTs up to approximately

2.2 and 1.8 percent, respectively, at the end of 2016. The major differences are observed in the short wavelength bands from M1 to M4 which had the largest correction from the lunar corrections. Other longer wavelength bands showed less than 1 percent level differences with M7 and M8 as shown in Figure 7. In addition, OC's lunar corrected SD F-factor (blue solid line) shows a very smooth lifetime trends compared to the operational and RSBAutoCal LUTs which have minor noisy responses in the lifetime trends.

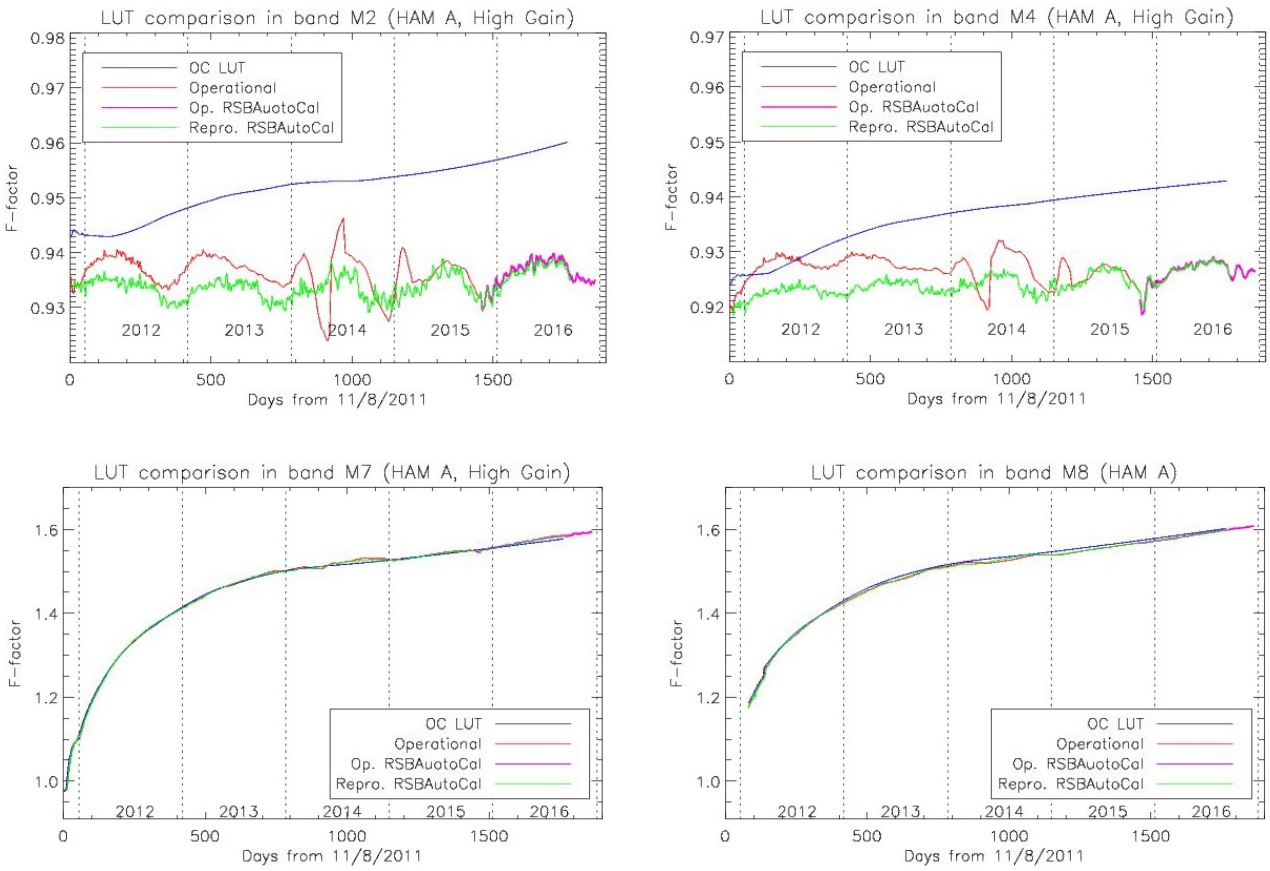

Figure 7. S-NPP VIIRS operational (red), operational RSBAutoCal (pink), reprocessing RSBAutocal (green), and OC reprocessing (blue) SD F-factors in bands M2, M4, M7 and M8.

The baseline VIIRS reprocessing is preformed using the standard RSBAutoCal LUT which is delivered with official ADL code. The F-factor ratio plots between reprocessing RSBAutoCal LUTs and operational LUTs are shown in Figure 8. First of all, the annual oscillation patterns between the 2012 and 2014 have been corrected which was caused by the solar vector problems in all bands. Secondly, the two H-factor (SD degradation) sudden changes were corrected especially in year 2014. Since the H-factors are only applicable to the bands M1~M7, these changes are observable in the left plot in Figure 8. The C0 equal to 0 update affected all RSB bands but it is mostly visible in band I3 as shown in the right plot in Figure 8 as a blue line. The biweekly manually delivered fast-track F-PREDICTED LUTs was switched to the IDPS implementation of RSBAutoCal on November of 2015. Starting from this point, the F-factor ratios are very close to unity in all bands. The small differences are caused by the RSBAutoCal algorithm implementation differences between the operational IDPS and independently processed ADL version.

Implementation of the OC F-factor LUT into the reprocessed VIIRS SDR

The S-NPP VIIRS SDR granules are reprocessed using baseline RSBAutoCal F-factors; however, there are long-term F-factor differences between the RSBAutoCal and OC F-factors in Figure 7. To mitigate the radiometric calibration differences, a 'RadiometricBiasCorrection' factor is inserted into the VIIRS SDR product as a field of HDF format as shown in Figure 8. This single correction factor is applicable to all observation in the given granule in all RSB bands with minimal effect to users. The 'RadiometricBiasCorrection' provides one reprocessed SDR granule with two different versions of calibration meeting different user's needs, which is very similar to OC's EDR ratio approach [26]. In Figure 8, the indices 0 and 1 are used for OC F-factor application and indices 2 and 3 are reserved for other user's application. The index 1 value holds the bias and the index 0 value holds the multiplicative factor to convert the radiance (or reflectance) from RSBAutoCal to OC version. The 'RadiometricBiasCorrection' factor is applicable to radiance and reflectance calculation.

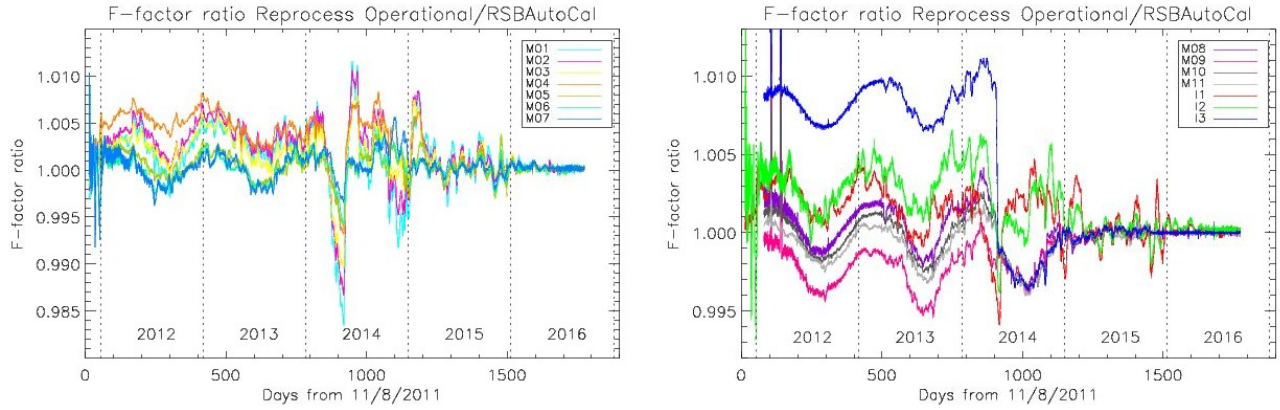

Figure 8. RSB F-factor ratio plot between Operational and RSBAutoCal LUTs.

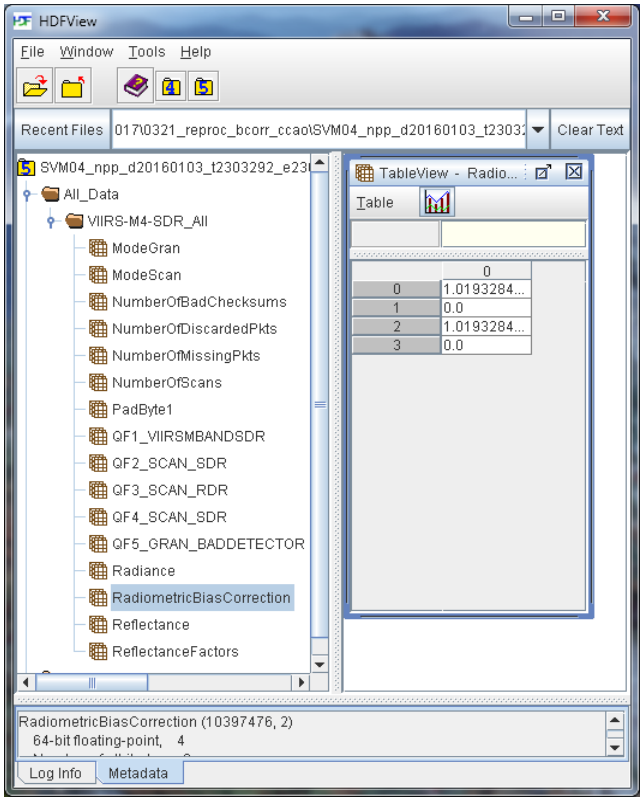

Figure 9. An example of the HDFView window for a VIIRS RSB granule in band M4 with the 'RadiometricBiasCoreection' field.

The 'RadiometricBiasCorrection' values are based on high gain state F-factors in dual gain bands. The long-term differences are obviously shown in the ratio plots in Figure 10 between the OC and Operational LUTs. Large F-factor differences are observed in the short wavelength bands M1 to M4. The long-term trends differences in these short wavelength bands are caused by fitting the SD F-actors to the lunar F-factors [18]. Other RSB bands M5 to M11 show quite consistent calibration in Figure 10. The band I1 and I3 have large differences up to 1 percent level in recent years. One of the possible reasons could be the C coefficient differences in the OC's F-factor calculation.

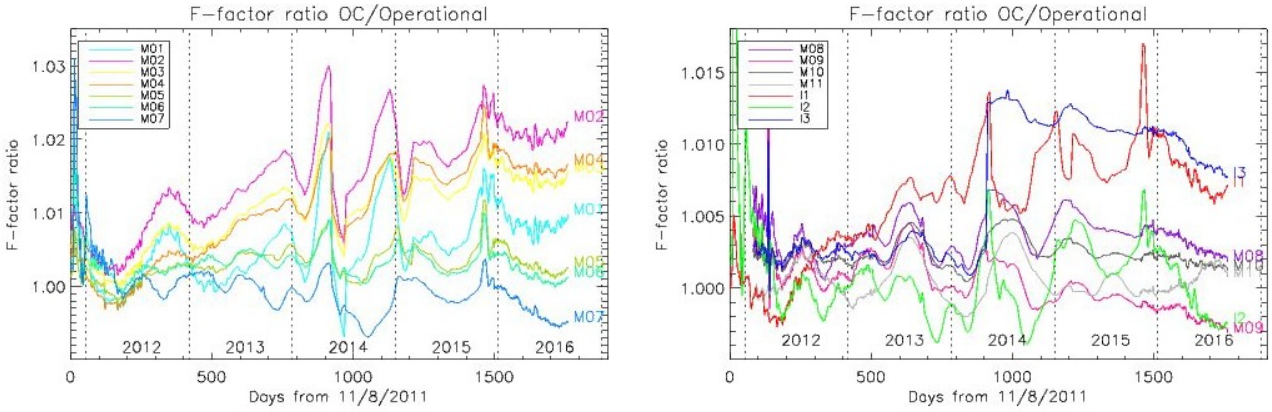

Figure 10. RSB F-factor ratio plot between OC and Operational LUTs

5. SUMMARY

This paper is a comprehensive report of the S-NPP VIIRS SDR reprocessing improvements in terms of RSB calibration and the EDR products especially with the OC applications. The reprocessed SDR products are produced by an offline software package called ADL version 4.2 with Mx 8.11, which includes accumulative updates over five years. As a major improvement, the primary RSB SDR products are generated by using the RSBAutoCal F-factor LUTs with an alternative option of converting to the OC group's calibration by applying the 'RadiometricBiasCorrection' factor. The reprocessed RSB SDR products are significantly improved by stabilizing the early lifetime calibration uncertainties, removing H/F-factor discontinuities, using a new set of C coefficients, correcting the solar vector, and applying new screen transmittance LUTs.

The OC LUTs remove the artificial seasonal oscillations and significantly reduces the noise in the SDR products generated by using the RSBAutoCal F-factor LUTs. They also remove the artificial long-term drifts in the SDR products. The OC LUTs significantly improve the accuracy of the SDR products and their long-term stability, the latter is most critical to the accuracy and quality of the EDR products.

Improvements have been made to the VIIRS SDR product with stable and consistent radiometric calibration. The sustained sensor characterization and calibration has enable to identify the calibration issues, resulting in the delivering well-calibrated SDR that continue to meet SDR and EDR requirements.

Acknowledgments

The manuscript contents are solely the opinions of the authors and do not constitute a statement of policy, decision, or position on behalf of NOAA or the U.S. government. This work is funded by the NOAA Joint Polar Satellite System (JPSS) program.

REFERENCES

[1] C. Cao, F. J. De Luccia, X. Xiong, R. Wolfe, and F. Weng, "Early on-orbit performance of the visible infrared imaging radiometer suite onboard the suomi national polar-orbiting partnership (S-NPP) satellite," *IEEE Trans. Geosci. Remote Sens.*, vol. 52, no. 2, pp. 1142–1156, 2014.

[2] C. Cao, J. Xiong, S. Blonski, Q. Liu, S. Uprety, X. Shao, Y. Bai, and F. Weng, "Suomi NPP VIIRS sensor data record verification, validation, and long-term performance monitoring," *J. Geophys. Res. Atmos.*, vol. 118, no. 20, pp. 11664–11678, 2013.

[3] T. J. Choi, N. Sun, W. Chen, C. Cao, F. Weng, E. Resource, T. Ert, and S. N. Noaa, "S-NPP VIIRS Significant Events in 2014 Monitored by NOAA ICVS Web-page," in *NOAA STAR JPSS 2015 Annual Science Team Meeting College Park, MD*, 2016.

[4] N. Baker, "Joint Polar Satellite System (JPSS) VIIRS Radiometric Calibration Algorithm Theoretical Basis Document (ATBD)," 2014.

[5] T. Choi, C. Cao, and F. Weng, "S-NPP VIIRS thermal emissive band gain correction during the blackbody warm-up-cool-down cycle," *Proc. SPIE - Int. Soc. Opt. Eng.*, vol. 9972, pp. 1–9, 2016.

[6] C. Cao, W. Wang, S. Blonski, and B. Zhang, "Radiometric traceability diagnosis and bias correction for the Suomi NPP VIIRS long-wave infrared channels during blackbody unsteady states," *J. Geophys. Res. Atmos.*, pp. 1–13, 2017.

[7] S. Lee, K. Chiang, X. Xiong, C. Sun, and S. Anderson, "The S-NPP VIIRS day-night band on-orbit calibration/characterization and current state of SDR products," *Remote Sens.*, vol. 6, no. 12, pp. 12427–12446, 2014.

[8] J. McIntire, D. Moyer, B. Efremova, H. Oudrari, and X. Xiong, "On-orbit characterization of S-NPP VIIRS transmission functions," *IEEE Trans. Geosci. Remote Sens.*, vol. 53, no. 5, pp. 2354–2365, 2015.

[9] J. Sun and M. Wang, "On-orbit calibration of Visible Infrared Imaging Radiometer Suite reflective solar bands and its challenges using a solar diffuser.," *Appl. Opt.*, vol. 54, no. 24, pp. 7210–23, 2015.

[10] X. Shao, C. Cao, and T. C. Liu, "Spectral dependent degradation of the solar diffuser on Suomi-NPP VIIRS due to Surface Roughness-induced Rayleigh Scattering," *Remote Sens.*, vol. 8, no. 3, 2016.

[11] J. Sun and M. Wang, "Visible Infrared Imaging Radiometer Suite solar diffuser calibration and its challenges using a solar diffuser stability monitor," *Appl. Opt.*, vol. 53, no. 36, pp. 8571–8584, 2014.
[12] J. Sun, M. Chu, and M. Wang, "Degradation nonuniformity in the solar diffuser bidirectional reflectance distribution function," *Appl. Opt.*, vol. 55, no. 22, pp. 6001–6016, 2016.
[13] J. Sun, X. Xiong, W. L. Barnes, and B. Guenther, "MODIS reflective solar band on-orbit lunar calibration," *IEEE Trans. Geosci. Remote Sens.*, vol. 45, no. 7, pp. 2383–2393, 2007.
[14] J. Sun, X. Xiong, and J. Butler, "NPP VIIRS On-Orbit Calibration and Characterization Using the," in *Society of Photo-Optical Instrumentation Engineers (SPIE) Conference Series*, 2012, vol. 8510, pp. 1–9.
[15] J. Sun and M. Wang, "Radiometric calibration of the Visible Infrared Imaging Radiometer Suite reflective solar bands with robust characterizations and hybrid calibration coefficients," *Appl. Opt.*, vol. 54, no. 31, p. 9331, 2015.
[16] T. Choi, C. Cao, F. Weng, and N. Star, "RADIOMETRIC STABILITY MONITORING OF THE S-NPP VIIRS OCEAN COLOR BANDS USING THE MOON," in *International Symposium on Remote Sensing*, 2016, pp. 1–4.
[17] T. Choi, X. Shao, C. Cao, and F. Weng, "Radiometric Stability Monitoring of the Suomi NPP Visible Infrared Imaging Radiometer Suite (VIIRS) Reflective Solar Bands Using the Moon," *Remote Sens.*, vol. 8, no. 1, p. 15, 2015.
[18] J. Sun and M. Wang, "VIIRS Reflective Solar Bands Calibration Progress and Its Impact on Ocean Color Products," *Remote Sens.*, vol. 8, no. 3, pp. 1–9, 2016.
[19] M. Wang, X. Liu, L. Jiang, S. Son, J. Sun, W. Shi, L. Tan, P. Naik, K. Mikelsons, X. Wang, and V. Lance, "Evaluation of VIIRS Ocean Color Products," in *Society of Photo-Optical Instrumentation Engineers (SPIE) Conference Series*, 2014, vol. 9261, pp. 1–15.
[20] F. Weng, "Joint Polar Ssatellite System Scientific Data Record Reprocessing Plan," in *NOAA Workshop on JPSS Life-Cycle Data Reprocessing to Advance Weather and Climate Applications May 17-18, 2016*, 2016.
[21] S. Blonski and C. Cao, "Suomi NPP VIIRS Reflective Solar Bands Operational Calibration Reprocessing," *Remote Sens.*, vol. 7, no. 12, pp. 16131–16149, 2015.
[22] D. Moyer, N. Vandermierden, K. Rausch, and F. De Luccia, "VIIRS reflective solar bands on-orbit calibration coefficient performance using imagery and moderate band intercomparisons," vol. 9223, p. 922305, 2014.
[23] J. Fulbright, S. Anderson, N. Lei, B. Efremova, Z. Wang, J. McIntire, K. Chiang, and X. Xiong, "The solar vector error within the SNPP Common GEO code, the correction, and the effects on the VIIRS SDR RSB calibration," vol. 9264, p. 92641T, 2014.
[24] E. Haas, D. Moyer, and F. De Luccia, "MAINTAINING SNPP VIIRS REFLECTIVE SOLAR BAND SENSOR DATA RECORD QUALITY: ON-ORBIT UPDATE OF SCREEN TRANSMISSION AND SOLAR DIFFUSER BRDF PARAMERS," in *In Proceedings of the 11th Symposium on New Generation Operational Environmental Satellite Systems, Phoenix, AZ, USA, 4–8 January 2015*, 2015.
[25] G. Moy, K. Rausch, E. Haas, T. Wilkinson, J. Cardema, and F. De Luccia, "Mission history of reflective solar band calibration performance of VIIRS," vol. 9607, p. 96071N, 2015.
[26] J. Sun, M. Wang, L. Tan, and L. Jiang, "An efficient approach for VIIRS RDR to SDR data processing," *IEEE Geosci. Remote Sens. Lett.*, vol. 11, no. 12, pp. 2037–2041, 2014.